Dams and Reservoirs under Changing Challenges – Schleiss & Boes (Eds)
© 2011 Taylor & Francis Group, London, ISBN 978-0-415-68267-1

Shaking table test of concrete dams with penetrated cracks and DEM analysis simulation

T. Iwashita, T. Kirinashizawa, Y. Yamaguchi & H. Kojima
Public Works Research Institute, Tsukuba, Japan

Y. Fujitsuka
CTI Engineering Co., Ltd., Fukuoka, Japan (Former Public Works Research Institute)

ABSTRACT: To evaluate the seismic performance of concrete gravity dams subjected to strong earthquakes such as the maximum credible earthquake, it is necessary to evaluate the seismic stability of the detached block of the dam body when tensile cracks in the dam body are predicted to penetrate from the upstream face to the downstream face. In this study, shaking table tests of a dam-shaped model specimen with penetrated cracks were performed considering hydraulic loading from the reservoir. The dynamic behavior of the detached block was analyzed using the pictures captured by a high-speed camera. The shaking table tests under two load conditions, with and without uplift pressure acting on the penetrated cracks, clarified the impact of uplift pressure on the behavior of the detached block. Numerical simulations of the dynamic behavior of the detached block during the shaking table tests were performed based on the Distinct Element Method (DEM).

1 INTRODUCTION

The Ministry of Land, Infrastructure, Transport and Tourism (MLIT) of Japan enacted "Guidelines for Seismic Performance Evaluation of Dams Against Large Earthquakes (Draft)" (River Bureau of the MLIT, 2005), which systematically regulates the method of evaluating the seismic performance of dams under the Level 2 earthquake, which is equivalent to the maximum credible earthquake, and has tentatively applied the guidelines to the dams under the jurisdiction of the MLIT. Under the guidelines, a dam is evaluated by confirming two seismic performance functions: (1) the storage function of the dam is maintained and (2) damage which has occurred is limited to a range which can be repaired. Regarding Function (1), earthquake response analysis considering the damage process is performed for a concrete dam, confirming that the damage which occurs is limited. In the case of a concrete gravity dam, conditions for tensile failure are generally critical for Function (1), which is considered to be satisfied if the tensile cracks generated in the dam body do not penetrate completely between the upstream and downstream faces. However, the guidelines also state that even when tensile cracks penetrate from the upstream to downstream faces of a dam body, if the upper detached block of the dam body is not unstable, it can be assumed that Function (1) is satisfied. Therefore, in a case where the earthquake response analysis shows that cracks penetrate from the upstream face to the downstream face, a more detailed evaluation by assessing the stability of the dam body after the dam body is separated by penetrated cracks.

Some researchers have studied the seismic performance of concrete dam bodies separated by the penetration of cracks. Malla & Wieland (2006), Zhu & Pekau (2007) and Wang (2008) used finite element analysis, and Pekau & Cui (2004) used the distinct element method (DEM) analysis, to evaluate the stability of dams separated by penetrated cracks by analyzing dynamic behavior, including rocking and sliding, of the upper detached concrete block. Most of these analyses were based on a case study of the Koyna Dam, which was a concrete gravity dam in which cracks penetrated between the upstream and downstream faces at the elevation

of the downstream gradient of the dam body changed due to the Koyna Earthquake of 1967. However, there have been almost no experimental studies, including shaking table tests, on the dynamic behavior of detached blocks due to penetrated cracks.

In this study, to clarify the seismic behavior of the detached block of a crack-penetrated dam body, shaking table tests were performed using a dam-shaped model specimen. The behavior of the upper detached block of the model in the shaking table tests was reproduced by DEM analysis.

2 SHAKING TABLE TESTS FOR DAM MODEL

2.1 *Experimental apparatus*

A water tank (1.25 m long, 0.5 m wide, and 0.8 m deep) was installed on the shaking table (8 m long and 8 m wide) and a dam-shaped model mortar specimen that had already been separated into two blocks was placed inside the water tank. The reservoir water level was kept at a constant depth of 465 mm during each shaking test by injecting water using a pump and letting it overflow from the weir as shown in Figure 1.

The dimensions of the dam model specimen are 515 mm in dam height, 318 mm in base length in the upstream-downstream direction and 300 mm in thickness in the dam axis direction. The upstream face of the specimen was vertical and the downstream slope had a gradient of 1:0.8. The model specimen assumed that cracks were generated along a horizontal construction joint at the lower elevation of the dam, where large tensile stress is generated during shaking, and that the cracks penetrated from the upstream to downstream face. The model specimen was made of mortar with a maximum aggregate size of 0.75 mm. The specimen was made by the following process. First, the lower part with a layer thickness of 115 mm was placed. One day later, after laitance clearance by wire brushing, remover was applied to the construction joint. Next, the upper part of the model specimen was placed. Seven days later, the model specimen was split into two blocks along the construction joint with remover.

The scale factor ($1/\lambda$) of the model specimen with a height of about 0.5 m corresponds to 1/30 for a prototype dam with a height of 15 m, and 1/200 for a 100 m-high prototype dam. Table 1 shows the relations of the properties of the prototype dam converted to the model scale based on the similarity rule with the material properties of the model specimen. The compressive strength of the mortar specimens was 3.94 N/mm^2, despite efforts to make low-strength mortar because of the limitation of removal of forms. The compressive strength and elastic modulus of the specimen are somewhat larger than those of prototype dams according to the similarity rule based on scale.

2.2 *Methodology of shaking table tests*

The shaking table tests were carried out for two cases with water pressure acting directly from the reservoir inside the penetrated crack of the model specimen (Cases-UPL-a and -b) and for one case in which water pressure acting directly from the reservoir was prevented (Case-N-UPL), as shown in Table 2. In Case-N-UPL, a latex sheet was loosely pasted on the upstream side of the penetrated crack, preventing reservoir water flowing from the upstream face into the penetrated crack and water pressure directly from the reservoir.

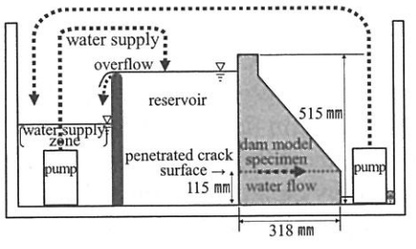

Figure 1. Schematic figure of the experimental apparatus.

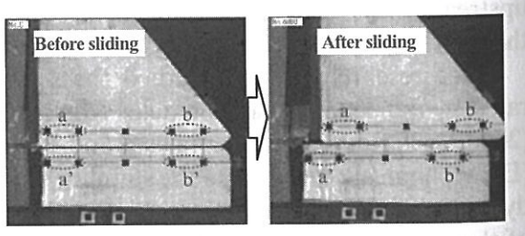

Photo 1. Pictures captured by a high-speed camera before and after sliding of the upper detached block.

Table 1. Relations of the similarity rule and material properties of the dam model specimen.

	Range of properties of prototype dam	Similarity ratio	Range of properties of prototype dam converted to model height of 0.5 m based on the similarity rule	Dam model specimens used for experimental tests
	(For dam height of 15 to 100 m)	(λ = 30 to 200)		(Dam model height of about 0.5 m)
	(a)	(b)	(a) × (b)	
Dam height	15 to 100 m	$1/\lambda$	–	About 0.5 m
Elastic modulus	20,000 to 30,000 N/mm^2	$1/\lambda$	100 to 1000 N/mm^2	6675 N/mm^2
Compressive strength	20 to 30 N/mm^2	$1/\lambda$	0.1 to 1.0 N/mm^2	3.94 N/mm^2

The shaking table was shaken with a sinusoidal acceleration with a frequency of 50 Hz which is equivalent to the range of 3.5 to 9.1 Hz for a prototype dam with a height of 15 to 100 m based on the similarity rule. The duration of the shaking acceleration was 5.5 seconds, and the acceleration amplitude increased linearly during the initial period of 0.5 second. The shaking test was performed as a series, with the amplitude of shaking increasing in steps of approximately 100 gal until reaching 800 to 1000 gal. The maximum input acceleration amplitude was equivalent to out of the range of Level 2 earthquake motions.

2.3 *Results of shaking table tests*

2.3.1 *Sliding displacement at each shaking step*

Photograph 1 shows pictures captured by a high-speed camera before and after sliding of the upper detached block. Figure 2 shows the relationship between the input shaking acceleration amplitude and residual horizontal relative displacement of the upper detached block relative to the lower block for each shaking step in all test cases. In Cases-UPL-a and -b, the sliding of the upper detached block significantly increases toward the downstream face when the input acceleration amplitude was 700 to 800 gal. But in Case-N-UPL in which water pressure from the reservoir was prevented from directly acting in the penetrated cracks, the sliding of the upper detached block significantly increased at the shaking step of 900 gal amplitude. When the upper detached block slides downstream in Case-N-UPL, the uplift acting on the penetrated crack surface near the upstream side is so small compared with that in Cases-UPL-a and -b that the upper detached block resists sliding, as mentioned in the next section.

2.3.2 *Behavior mechanism of upper detached block*

The typical dynamic behavior of the upper detached block was analyzed from observations of the final shaking step (input amplitude acceleration of about 970 gal) in Case-UPL-b. Figure 3 shows the horizontal acceleration time history of the lower block of the model specimen and the horizontal relative displacement time history at the bottom of the upper detached block relative to the lower block. The upper detached block slid gradually downstream after the acceleration time history of the lower block reached a constant amplitude of the shaking.

Figure 4 shows an enlargement for the period from 4.0 to 4.1 seconds in Case-UPL-b shown in Figure 3. Figure 5 shows the behavior of the detached block in the period from 6.0 to 6.1 seconds in Case-N-UPL. Tracking analysis using the pictures captured by a high-speed camera with a shutter speed of 1000 frames per second was performed to obtain the dynamic 2D-behavior of the rigid upper detached block. Comparing the vertical relative displacement of the upper detached block on the upstream side (DH-Y1 indicates vertical length between

Table 2. Test condition of shaking cases.

Case	Uplift pressure acting on the penetrated crack surface	Frequency of sinusoidal acceleration input
Case-UPL-a Case-UPL-b	With uplift pressure	50 Hz
Case-N-UPL	Without uplift pressure*	50 Hz

*Water pressure from the reservoir was prevented from acting directly on the penetrated crack surface.

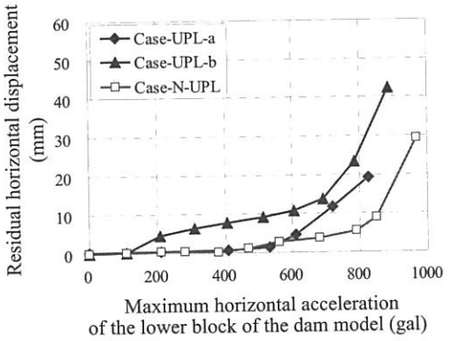

Figure 2. Residual horizontal relative displacement at each shaking step.

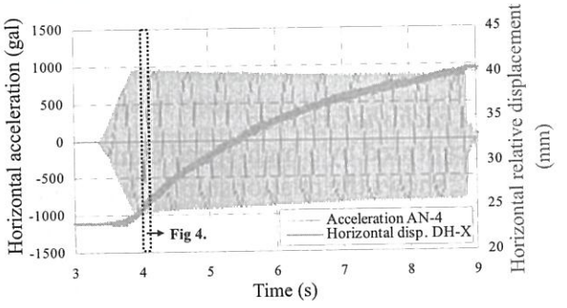

Figure 3. Horizontal acceleration time history of the lower block and horizontal relative displacement time history of the upper detached block (Final shaking step in Case-UPL-b).

a-a' in Photo. 1) with that on the downstream side (DH-Y2 indicates vertical length between b-b' in Photo. 1), we can see the displacement time histories of DH-Y1 and DH-Y2 with a reverse phase. We can thus identify the rocking of the upper detached block. The rocking motion was partitioned into tilting toward the downstream side (rocking motion I) and toward the upstream side (rocking motion II). Figures 4 and 5 are hatched to distinguish the period during rocking motions I and II. While rocking in the upstream and downstream directions, the upper detached block slid downstream a little at a time, as clearly shown by the horizontal displacement time history of DH-X. While the hydrodynamic pressure acting on the upstream face increased, the upper detached block slid downstream, with the penetrated crack on the downstream side closed and the detached block tilted downstream.

Next, the effect of the uplift pressure acting on the penetrated crack surface on the behavior of the model specimen is considered. In the test case in which water is permitted to flow from the reservoir into the penetrated surface (Case-UPL-b shown in Fig. 4), when the inertia force acted on the upper detached block in the downstream direction, uplift pressure of about 8 to 10 kPa acted instantaneously at PB-1 and PB-2 on the penetrated surface. In the same period, the upper block returned to its original position after tilting upstream (rocking motion II),

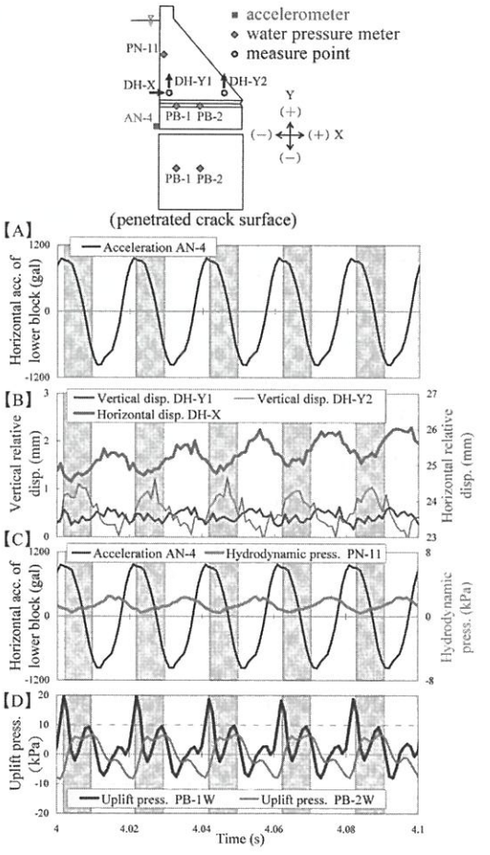

Figure 4. Measured value time histories of the behavior of the upper detached block (Final shaking step in Case-UPL-b).

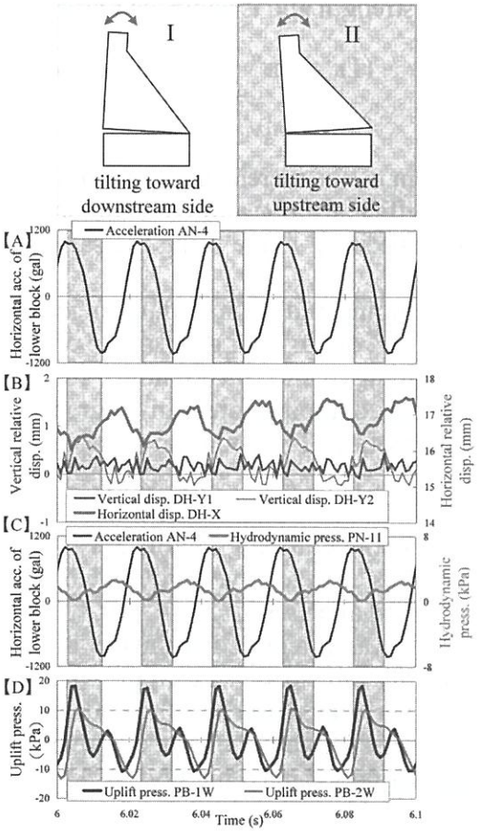

Figure 5. Measured value time histories of the behavior of the upper detached block (Final shaking step in Case-N-UPL).

the penetrated crack closed, and rocking motion I started to occur. It is assumed that because the action of this uplift pressure reduced the frictional resistance between the penetrated crack surfaces, the upper detached block slid easily downstream. On the other hand, in the case in which water pressure from the reservoir was prevented from acting on the penetrated crack surface (Case-N-UPL shown in Fig. 5), water gathered between the crack surface, even though direct seepage flow was prevented. Therefore, the rocking behavior of the upper detached block caused the pore water pressure between the penetrated surfaces as shown in Figure 5 [D]. When the inertia force acted on the detached block in the downstream direction, the uplift pressure near the upstream side in Case-N-UPL was significantly smaller than that in Case-UPL as shown in Figures 4 [D] and 5 [D]. As a result of this effect of uplift pressure, the sliding displacement in Case-N-UPL is seemed to be smaller than that in Case-UPL.

3 NUMERICAL SIMULATION

3.1 *Methodology of numerical analysis*

Numerical simulation of the dynamic behavior of the upper detached block during the shaking table tests was performed using the distinct element method (DEM) with the UDEC code (Itasca, 2004). The analysis model mesh is shown in Figure 6. Table 3 shows the material properties of the analysis model. The material properties were set from the experimental tests for mortar specimen with the same mix proportion and age as the dam model specimens used for the shaking table tests.

Interface elements were set in the normal direction and in the tangential direction as the joint model between the penetrated crack surfaces of the analysis model. While the upper detached block and the lower block are in contact, the normal stress σ_n acting between the upper and lower blocks is transmitted through a constant normal stiffness k_n. This is the soft contact assumption. The constant normal stiffness k_n was set based on the elastic modulus of the mortar of the specimen. In the shear direction along the penetrated surface, the Coulomb slip model was adopted in UDEC. The shear stress τ_s is limited by the shear strength τ_f which is a combination of cohesive (C) and frictional (φ) strength and is controlled by a constant shear stiffness k_s:

If $\tau_s < C + \sigma_n \tan\varphi = \tau_f$ (1), then $\Delta\tau_s = -k_s \Delta u^e s$ (2)

and if $\tau_s \geq \tau_f$ (3), then $\tau_s = \tau_f$ (4)

where Δu^e_s is the elastic component of the incremental horizontal relative shear displacement.

The cohesion C, frictional coefficient $\tan\varphi$ and constant shear stiffness k_s were obtained from the box shear tests of the specimen made using the same mortar mix proportion and age, as shown in Table 3.

A combination of Rayleigh damping and stiffness damping force was adopted as damping. The Rayleigh damping factor of 15% or 20% was given at the predominant input frequency of 50 Hz considering radiation damping due to the boundary condition with a rigid basement. The method of setting the stiffness damping forces gives greater control for simulating the block bounce including rocking motion. The equation for the stiffness damping force is:

$$f = -\beta \times K \times l \times \Delta v \tag{5}$$

where f is the damping force; β is the damping factor; K is stiffness; l is length of contact on the penetrated surface; and Δv is change in velocity. The damping factor of 1.0×10^{-4} or 1.2×10^{-4} was given in the numerical analyses.

The sinusoidal velocity, which was integrated from the input acceleration wave with a frequency of 50 Hz in the shaking table test, was input. The numerical analysis at all the shaking steps was continuously performed starting from an input acceleration with amplitude of 300 gal. Hydrodynamic pressure acting on the upstream face of the model specimen was calculated using Westergaard's added mass method.

The analysis cases are shown in Table 4. The damping factor was adjusted by the numerical analyses of Cases N-1 to N-3 which were performed without uplift pressure on the penetrated crack. Cases U-1 to U-3 were performed with uplift pressure acting on the penetrated crack

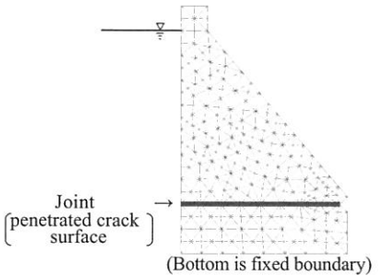

Figure 6. DEM analysis mesh of the model.

Table 3. Material properties of the analysis model.

	Material properties	
Upper and lower blocks	Density ρ	2090 kg/m^3
	Dynamic elastic modulus E	6700 N/mm^2
	Poisson's ratio ν	0.2
Penetrated crack surface	Cohesion C	0.0304 N/mm^2
	Coefficient of friction tanφ	0.82
	Normal stiffness k_n	6700 N/mm^2/m
	Shear stiffness k_s	590 N/mm^2/m

Table 4. Cases of numerical analysis.

Case	Condition of uplift	Rayleigh damping factor	Stiffness damping factor
Case N-1	Without uplift pressure	15%	1.0×10^{-4}
Case N-2		15%	1.2×10^{-4}
Case N-3		20%	1.0×10^{-4}
Case U-1	With uplift pressure*	15%	1.0×10^{-4}
Case U-2		15%	1.2×10^{-4}
Case U-3		20%	1.0×10^{-4}

*Static uplift pressure was made to act on the nodes of the penetrated crack joint.

surface. The triangle-shape distribution of static uplift pressure measured on the penetrated surface in the model specimen before shaking was given instead of the dynamic uplift pressure for the numerical analyses of Cases U-1 to U-3.

3.2 *Results of numerical analysis*

3.2.1 *Rocking motion of the upper detached block*

Figure 7 shows a part of the time history results of the experimental shaking table test (Case-N-UPL) and the numerical analyses (Cases N-1 to N-3) performed without uplift pressure for the final shaking step of 900 to 970 gal. The experimental test results in Figure 7 (1) show that the rocking motion of the upper detached block was such that the upper block tilted upstream and returned to the normal position (the penetrated surface of the downstream side closed) and then the block tilted downstream (the penetrated surface of the upstream side opened), while the upper block slid downstream. In the numerical analysis results in Figure 7 (2) and (3), the time histories of vertical displacement of the detached block on the upstream side are reverse phase with those on the downstream side. The behavior of the detached block in the numerical analyses reproducibly simulated the rocking behavior observed in the experimental test Case-N-UPL. The vertical displacement amplitudes of the block, which is the opening gap of the penetrated surface, of the analyses Cases N-2

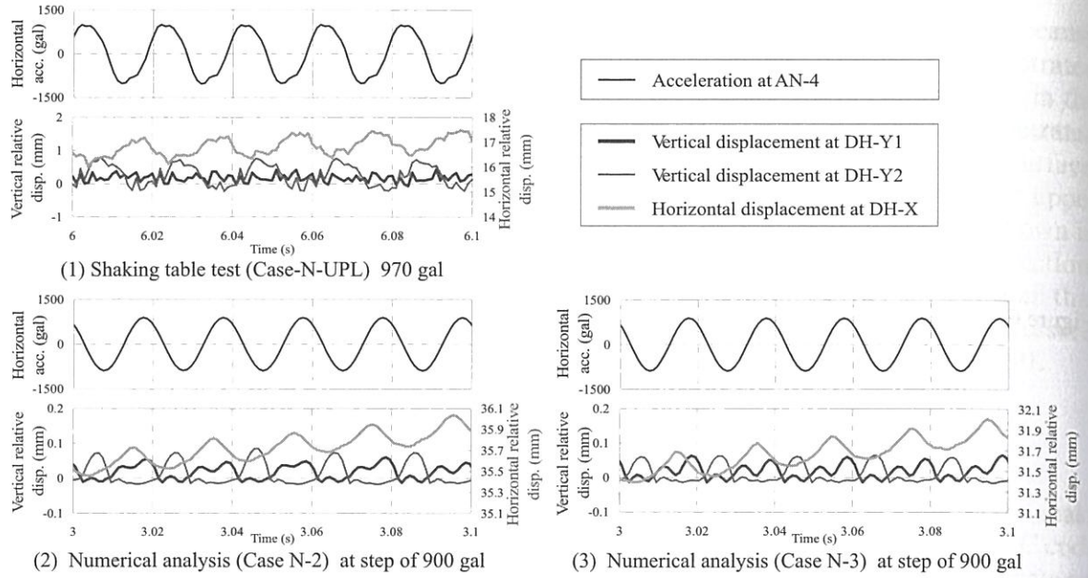

Figure 7. Measured value time histories of the behavior of the upper detached block.

and N-3 in Figure 7 (2) and (3) are quantitatively smaller than that of the experimental test Case-N-UPL in Figure 7 (1). The reason is expected to be because of the modeling of the penetrated surface of the specimen. The penetrated surface of the specimen has asperities due to the mortar aggregate. These asperities caught the upper detached block during rocking, causing the rocking amplitude to increase. On the other hand, the penetrated surface in the numerical analysis was modeled as a flat surface with frictional resistance based on the soft contact assumption.

3.2.2 *Horizontal displacement of the upper detached block*

The upper detached block slid toward the downstream side, vibrating in the upstream-downstream directions in both of the experimental shaking test (Case-N-UPL) and the numerical analyses (Cases N-2 and N-3) in Figure 7. The amplitudes of horizontal displacement time histories of the block in the numerical analyses were about half those of the experimental test results.

Figure 8 shows the residual horizontal displacement at each shaking step for numerical analyses Cases N-1 to N-3 without uplift pressure. In the numerical analysis results, the upper block started to slide at the shaking step with an acceleration amplitude of about 600 gal, which is similar to the behavior during the experimental test of Case-N-UPL. Though the residual horizontal displacements in Cases N-1 to N-3 become slightly larger than in the experimental test Case-N-UPL with subsequent shaking steps, the increase tendency for the residual displacement in Cases N-2 and N-3 to increase with larger damping factor is similar to that in Case-N-UPL.

Figure 9 shows the experimental results of Cases-UPL-a and -b, and numerical analysis results of Cases U-1 to U-3, in which uplift pressure acted on the penetrated crack surface. In Cases U-1 to U-3, the upper block started to slide at the shaking step with an acceleration amplitude of about 600 gal, which is similar to the behavior during Case-UPL-a. The residual horizontal displacements in Cases U-1 to U-3 become slightly larger than those in Cases-UPL-a and -b with subsequent shaking steps. Regarding the numerical analysis cases with uplift pressure (Case U series) in Figure 9 compared with the cases without uplift pressure (Case N series) in Figure 8, the residual horizontal displacements for Cases U series are somewhat larger than those for Cases N series in each case under the same damping conditions. The uplift pressure acting on the penetrated crack surface reduce the frictional resistance acting on it. The distribution of the static uplift pressure measured on the penetrated surface before shaking was given to the nodes of the penetrated surface of the DEM analysis model. Because the dynamic

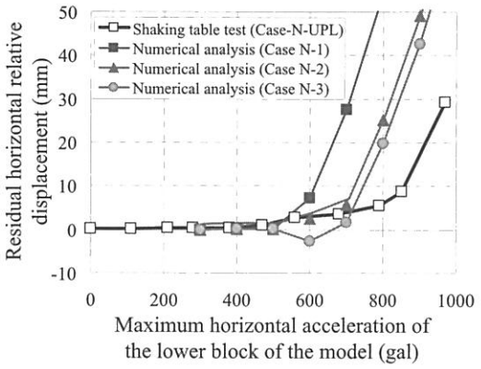

Figure 8. Residual horizontal relative displacement at each shaking step (Without uplift pressure).

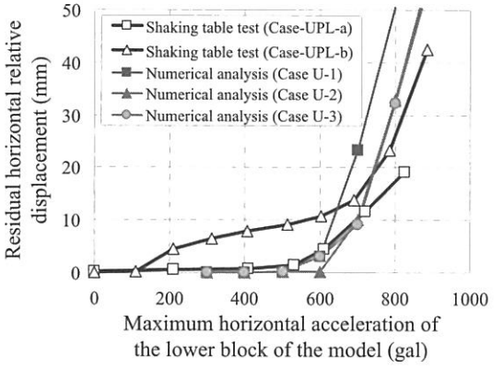

Figure 9. Residual horizontal relative displacement at each shaking step (With uplift pressure).

uplift pressure acts on the penetrated surface in the experimental tests Cases-UPL-a and -b shown in Figure 4, the uplift pressure input in the numerical analysis was different from the uplift pressure time history in the experimental tests. This is assumed to be one of the reasons for the difference of the residual horizontal displacements between Cases-UPL-a and -b and Cases U-1 to U-3, though the damping factors affect the results of the numerical analysis.

In the next step of this study, it will be necessary to improve the setting of input uplift pressure, stiffness and strength on the interface of the penetrated crack for DEM analysis.

4 CONCLUSIONS

To evaluate the ultimate seismic resistance of a concrete gravity dam which cracks formed and penetrated the horizontal construction joint separating it into two parts, shaking table tests were performed using dam-shaped model mortar specimens. The following results were obtained by the experimental shaking table tests. Numerical simulations of the behavior of the detached block during the shaking table tests were performed by DEM analysis.

- The dynamic behavior of the upper detached block during strong shaking was measured and analyzed by the shaking table tests. When shaking acceleration in the upstream direction acted on the lower block, inertia force in the downstream direction acted on the upper detached block. Therefore, the upper detached block slid downstream, accompanying the rocking motion as the behavior changed from upstream side tilting to downstream side tilting. Conversely, when the inertia force in the upstream direction acted on the upper detached block, the detached block returned slightly upstream, accompanying the contrary rocking motion as the behavior changed from downstream side tilting to upstream side tilting. During shaking, horizontal relative displacement of the upper detached block

relative to the lower block occurred gradually in the downstream direction, with the upper block repeating the above-mentioned behavior.

- Comparable shaking table tests were performed under the loading conditions with or without uplift pressure acting on the penetrated crack surface. When the inertia force acted on the detached block in the downstream direction, the uplift pressure on the penetrated crack surface acted near the upstream face side. As a result, the shear resistance of the penetrated surface decreased and the upper detached block could easily slide in the downstream direction.
- A DEM simulation analysis of the dam model with a penetrated crack during the experimental shaking table tests was performed. The numerical analysis results roughly reproduced the rocking motion and residual horizontal displacement of the upper detached block during shaking, even though simple procedures were used, such as joint modeling for the penetrated surface and uplift pressure loading methods.

REFERENCES

Itasca Consulting Group, Inc. 2004. *Universal Distinct Element Code (UDEC) Theory and Background.*

Malla, S. & Wieland, M. 2006. Dynamic stability of detached concrete blocks in arch dam subjected to strong ground shaking. *First European Conference on Earthquake Engineering and Seismology, Geneva, 4–8 September 2006*: K10.

Pekau, O.A. & Cui, Y.Z. 2004. Failure analysis of fractured dams during earthquakes by DEM. *Engineering Structures* 26: 1483–1502.

River Bureau, Japanese Ministry of Land, Infrastructure, Transport and Tourism. 2005. Guidelines for Seismic Performance Evaluation of Dams against Large Earthquakes (Draft).

Wang, H. 2008. Seismic stability of detached concrete block of concrete gravity dam. *The 14th World Conference on Earthquake Engineering, Beijing, 12–17 October 2008*: S13–030.

Zhu, X. & Pekau, O.A. 2007. Seismic behavior of concrete gravity dams with penetrated cracks and equivalent impact damping. *Engineering Structures* 29: 336–345.